



HAL
open science

Thermally driven asymmetric responses of grains versus spin-glass related distributions of blocking temperature in exchange biased Co/IrMn bilayers

Vincent Baltz

► **To cite this version:**

Vincent Baltz. Thermally driven asymmetric responses of grains versus spin-glass related distributions of blocking temperature in exchange biased Co/IrMn bilayers. *Applied Physics Letters*, 2013, 102, pp.062410. 10.1063/1.4792347 . hal-01683658

HAL Id: hal-01683658

<https://hal.science/hal-01683658>

Submitted on 19 May 2019

HAL is a multi-disciplinary open access archive for the deposit and dissemination of scientific research documents, whether they are published or not. The documents may come from teaching and research institutions in France or abroad, or from public or private research centers.

L'archive ouverte pluridisciplinaire **HAL**, est destinée au dépôt et à la diffusion de documents scientifiques de niveau recherche, publiés ou non, émanant des établissements d'enseignement et de recherche français ou étrangers, des laboratoires publics ou privés.

Thermally driven asymmetric responses of grains versus spin-glass related distributions of blocking temperature in exchange biased Co/IrMn bilayers

V. Baltz^{a)}

SPINTEC, UMR 8191 CNRS/INAC-CEA/UJF-Grenoble 1/Grenoble-INP, F-38054 Cedex, France

(Received 20 November 2012; accepted 1 February 2013; published online 13 February 2013)

Controlling ferromagnetic/antiferromagnetic blocking temperatures in exchange biased based devices appears crucial for applications. The blocking temperature is ascribed to the ability of both antiferromagnetic grains and interfacial spin-glass-like phases to withstand ferromagnetic magnetization reversal. To better understand the respective contributions of grains versus spin-glass, blocking temperature distributions were measured after various thermal treatments for cobalt/iridium-manganese bilayers. The high-temperature contribution linked to antiferromagnetic grains shifts towards lower temperatures above a threshold thermal annealing. In contrast, the occurrence and evolution of training effects for the low-temperature contribution only agree with its inferred interfacial spin-glass-like origin. © 2013 American Institute of Physics. [<http://dx.doi.org/10.1063/1.4792347>]

Exchange bias (EB) refers to the exchange coupling between a ferromagnet (F) and an antiferromagnet (AF)^{1,2} and defines the reference direction required for the spin of conduction electrons in spintronics applications such as magnetic random access memories (MRAMs), sensors, logic devices, and radiofrequency emitters.³ In addition to that, thermally assisted (TA) MRAMs use EB in order to store data at room temperature (T) and to write binary data by elevation of T above the blocking temperature (T_B) and subsequent cooling with either positive or negative induced field. It is thereby essential to fully understand the EB phenomenon and in particular T_B and their dispersions (DT_B) for TA-MRAM applications. Since the first study on EB,⁴ most authors now agree that, for F/AF thin films, EB is ascribed to the ability of both AF grains (domains)^{5–12} and AF interfacial spin-glass-like phases^{8–18} to withstand F magnetization reversal. Although a substantial number of works have been reported, the respective contributions of grains versus interfacial spin-glass are still controversial and the concomitant mastering of the effect is still partial. It would become less so by systematically carrying out simultaneous observations, hitherto rarely completed.^{9–12} The specific procedure commonly carried out for measurements of DT_B above 300 K combined with the alternative use of a sufficiently low reference T recently provided a method for the above purpose.⁹ The present study focuses on the responses of the DT_B contributions to gradual annealing, which are expected to modify the layers properties above a threshold T.^{19,20} Owing to the various origins presumed for the two contributions to DT_B : grains versus interfacial spin-glass, distinct responses are expected, thereby possibly supporting their different causes and providing an additional knob for their respective understanding and control.

In this work, Ta(3 nm)/Cu(3 nm)/Co(3 nm)/IrMn(7 nm)/Pt(2 nm) are sequentially deposited at room-T by DC-magnetron sputtering onto a thermally oxidised silicon substrate.⁹ IrMn is made from an Ir₂₀Mn₈₀ target. A static

positive magnetic field of 2.5 kOe is applied in the sample plane during the entire deposition process. It is large enough to saturate the magnetization of the Co layer during the deposition of the IrMn layer. Therefore, all the growing AF entities with T_B higher than the deposition-T orient toward the positive direction.⁹ Applying a field *ab initio* does not require post-deposition field cooling (FC) to set EB, so it provides a reference as-deposited sample. After deposition, the sample is cut up into pieces subject to a positive FC from an initial annealing temperature (T_{init}) down to 4 K. The field (H_{FC}) applied during cooling stands along the direction of the *ab initio* field and, similarly, is large enough to saturate the Co layer. For the various sample pieces, T_{init} is respectively equal to 300 (i.e., ~no post-deposition annealing), 450, 550, 650, and 750 K. Following the initial FC, DT_B in the range of 4 K to T_{init} is deduced from hysteresis loops measured with a superconducting quantum interference device (SQUID). All the loops are performed at 4 K after a specific procedure, which involves FC from incremental annealing temperatures (T_a).^{7,9} Since the T in the SQUID can only reach 400 K, for T_{init} and T_a larger than 400 K, the samples are first FC in a furnace from T_{init} (T_a) down to room-T and then FC in the SQUID from 300 to 4 K. Since room-T was not exceeding 300 K during the experimental period, any effect of a minor loop due to the zero field transfer at room-T is expected to be reset when cooling from 300 to 4 K in the SQUID.

Typical hysteresis loops are shown in Fig. 1 for $T_{init} = 550$ K. After initial positive FC from T_{init} to 4 K, all the AF entities contributing to EB orient toward the positive direction. This leads to maximum loop shift for $T_a = 4$ K. From this initial state, the procedure consists in gradually reorienting the AF entities by use of negative FC down to 4 K from incremental T_a .^{7,9} The AF entities with T_B lower than T_a reverse. After each increment of T_a , a loop is measured at 4 K. Its shift in field (H_E) is proportional to the difference between pinned AF entities oriented positively and negatively. A gradual change in the amplitude and sign of H_E is observed in Fig. 1, since the higher the T_a , the more

^{a)}Electronic mail: vincent.baltz@cea.fr.

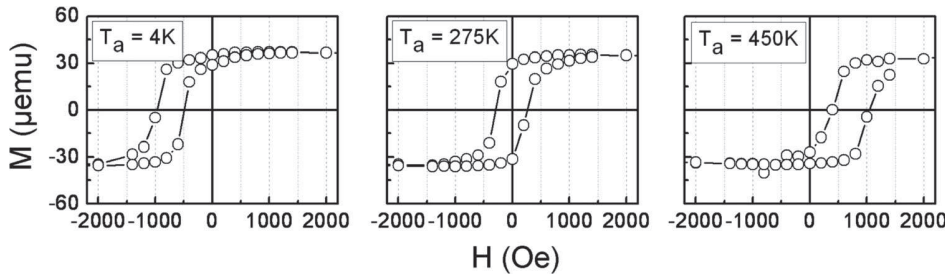


FIG. 1. Typical hysteresis loops measured at 4 K by SQUID along the FC direction, for a film of Ta(3 nm)/Cu(3 nm)/Co(3 nm)/IrMn(7 nm)/Pt(2 nm) subject to a procedure detailed within the text and involving various annealing temperatures (T_a).

reversed entities. H_E recovers its maximum around the maximum T_B , here 450 K, but with opposite sign, as a result of the reorientation of all the AF entities.

The variations of coercivity, H_C and loop shift, H_E with T_a are plotted in Fig. 2 for the various T_{init} . For some T_a , hysteresis loops are measured few consecutive times to probe potential training effects.^{21,22} To ease the reading, the concomitant data points are only plotted when relevant, i.e., when H_E and H_C vary from loop number n to $n+1$. Although it is accepted that training effects are triggered by F cycling and refer to the macroscopic signature of the rearrangement of the AF spin configuration toward equilibrium, the underlying microscopic mechanisms may be diverse. The effect has usually been considered as a rearrangement of AF

domains^{16,21} and could be derived in a phenomenological description that considers an associated order parameter for the AF interfacial magnetization.²³ The above descriptions lead to a square root decrease of H_E with n . Alternatively, some studies have shown that the sole AF symmetry could account for rearrangements.^{16,21} In this latter picture, symmetry induced training effects vanish after two loops, but “usual” training may take over afterwards.¹⁶ Here, from Fig. 2, no training was observed for $T_{init} \leq 550$ K. In contrast, for higher T_{init} (650 and 750 K), the differences between 1st and 2nd loops—see Fig. 3(a)—clearly highlight training. Figure 2 also shows that, for $T_{init} \leq 550$ K and within the experimental error, H_C is independent of T_a . This is expected since all the loops are measured at the same T . However, for $T_{init} \geq 650$ K, due to training as detailed below, the 1st loop H_C increases up to $T_a \sim 75$ K and then levels out. After the 2nd loop, H_C recovers its independence on T_a , which indicates that training has vanished. This agrees with the fact that no training was observed for further loops. As a consequence of the dissimilar variations of H_C with T_a for the 1st and 2nd loops, the difference between the two increases when T_a raises and then levels out at ~ 75 K, see Fig. 3(b). As also shown in Fig. 3(b), H_E shows similar trends. Training effects thus seem to be related here to anything that responds at low-T. Taking into account the presumed AF interfacial spin-glass-like origin of the low-T contribution to DT_B ,^{9,13} the following scenario can be suggested. First, when T_a increases, there is a rise of the amount of AF interfacial spin-glass phases sensitive to training and dragged along during the first F cycling, since more spin-glasses with T_B comprised between 4 K and T_a are reversed. In accordance with the training effect phenomenological picture,^{16,21–23} these spins are probably initially in a high energy metastable state. Then, training levels out when T_a reaches the spin-glasses maximum T_B , i.e., beyond the low-T contribution to DT_B . In accordance, the spin-glass maximum T_B corresponds to around 75 K, as can be seen in Fig. 4(b). Finally, above the spin-glass maximum T_B , the amount of spin-glass contributing to training is maximum, since all the spin-glasses subject to being dragged are then involved whatever T_a . When T_a reaches higher T it comes to additionally repining AF spins of full grains due to the granular origin of the high-T contribution to DT_B . The AF grains here certainly stand in a more stable repined magnetic configuration less prone to training since another increase in training is not observed. The fact that training occurs above $T_{init} = 650$ K means that the spin-glass phases became more sensitive to reorientation as a likely consequence of thermally activated intermixing and subsequent modifications of some layers properties.^{19,20}

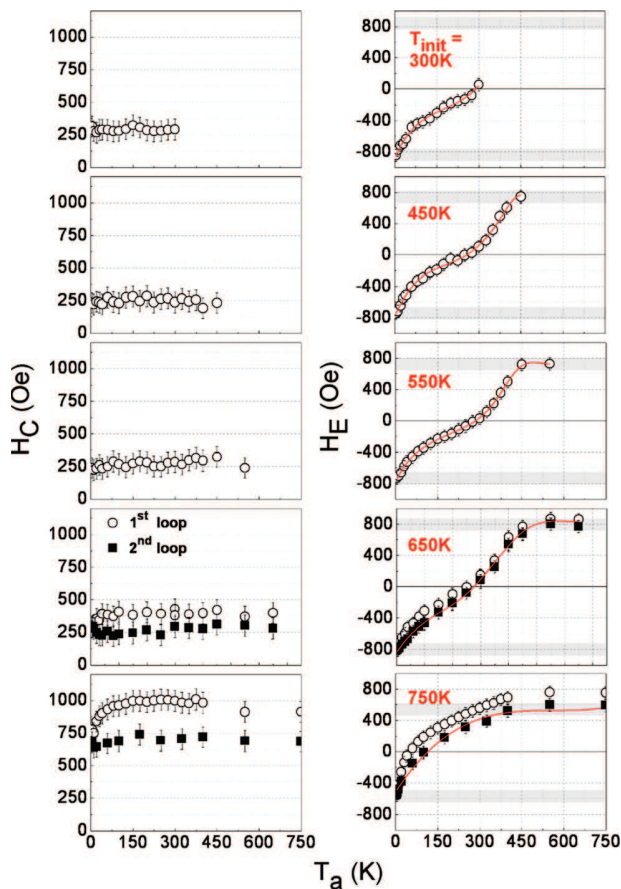


FIG. 2. Variations with T_a of the coercive field (H_C) and loop shift (H_E) deduced from hysteresis loops measured at 4 K (Fig. 1) for pieces of the same film subject to various initial temperatures (T_{init}). The notations 1st and 2nd refer to consecutive loops recorded at 4 K. The full lines result from interpolation of the data. The grey areas represent, within the experimental error, the minimum value of H_E ($H_{E,min}$) determined experimentally and the expected maximum value ($H_{E,max}$) calculated from: $H_{E,max} = -H_{E,min}$.

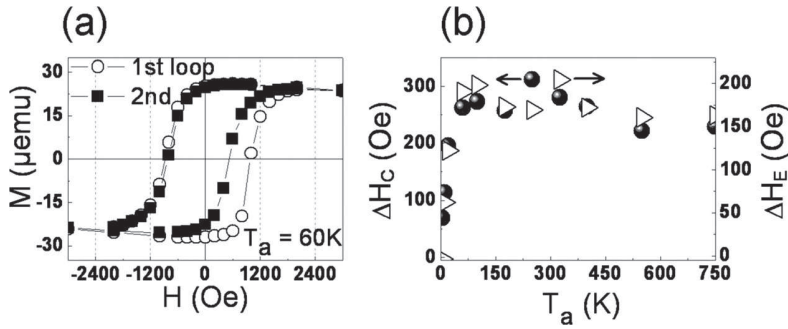


FIG. 3. For $T_{\text{init}} = 750$ K: (a) two successive hysteresis loops for $T_a = 60$ K and (b) variations with T_a of the differences of H_C and of H_E between 1st and 2nd loops.

Back to the mechanism at the origin of training: an isolated spin-glass-like phase shows no symmetry and therefore is not prone to training induced by symmetry.^{16,22} With that regards and taking into account that H_E vanishes here after two loops, it might well be that the origin of training is the “usual” thermal training discussed further up, which dies off quickly notably because the T_B of these spin-glasses is small compared to the measurement T of 4 K.²⁴ In addition, despite the inherent random and thus isotropic character of an isolated spin-glass, the coupling to the AF spin lattice underneath for F/AF systems likely brings anisotropy and preferential axes, thus lowering the energy of some arrangements of the spin-glass-like phase. Training induced by the AF symmetry and which is characteristic of a training that vanishes after two loops may be an alternative explanation. Let me then develop this in the framework of the model suggested in Ref. 22 for biaxial anisotropy AF like IrMn: some initially noncollinear ($\sim 90^\circ$) AF spins relax into an energetically more favourable collinear and antiparallel arrangement ($\sim 180^\circ$) after the first F reversal. For a field applied at an angle ϕ from one of the AF easy axes, the condition for training, i.e., the condition for initial $\sim 90^\circ$ arrangement of AF spins as opposed to initial antiparallel alignment and no training otherwise, is given by the following equation:²²

$$\left| \frac{J_{F-AF} + \varepsilon_{FC}}{J_{AF}} \cdot \frac{M_F}{M_{AF}} \cdot \frac{t_F}{t_{AF}} \right| > \frac{1}{\cos(\phi) + \sin(\phi)} \quad (1)$$

where J_{F-AF} is the interfacial exchange energy per unit surface between F and AF spins, J_{AF} is the exchange energy per unit surface between AF spins, M_F and M_{AF} are the respective magnetizations per unit volume of the sublattices, t_F and t_{AF} are the respective thicknesses, and ε_{FC} is the Zeeman energy per unit surface during FC: $\varepsilon_{FC} = H_{FC} \cdot M_F \cdot t_F$. The grains show no training thus Eq. (1) is in all likelihood not fulfilled, since

t_{AF} is probably too large. Instead, interfacial AF spin-glass phases could fulfil Eq. (1), due to their smaller effective thicknesses. The fact that training only occurs above $T_{\text{init}} = 650$ K, means that Eq. (1) then becomes fulfilled. More specifically, for high T_{init} , the ratio $(J_{F-AF} + H_{FC} \cdot M_F \cdot t_F) \cdot M_F \cdot t_F / (J_{AF} \cdot M_{AF} \cdot t_{AF})$ increases, as a likely consequence of thermally activated layers intermixing.^{19,20} Although definite values of J_{F-AF} , J_{AF} , and M_{AF} are not straightforwardly accessible to experiments, the other values can be measured and trends can then be assessed. H_{FC} stays the same. M_F is extracted from the SQUID data. For $T_{\text{init}} \leq 650$ K, $M_F \sim 1300 \text{ emu cm}^{-3}$ and it reduces to about 900 emu cm^{-3} for $T_{\text{init}} = 750$ K. Taking this into account for the explanation of the above ratio reduction, it implies that: (i) the higher the T_{init} , the much larger the J_{F-AF} ; this is unlikely since layers intermixing usually results in less F-AF exchange bonds, which inversely reduces the effective J_{F-AF} ; or (ii) the product $J_{AF} \cdot M_{AF}$ drops, which is much more likely, as will be confirmed below. Additionally, it is noteworthy that, within the experimental error, the maximum values of H_E and H_C , i.e., for $T_a = 4$ K in Fig. 2, are independent of T_{init} ($H_E \sim 800$ Oe and $H_C \sim 250$ Oe) except for $T_{\text{init}} = 750$ K, for which H_E reduces to 600 Oe and H_C rises to 600 Oe. H_E relates to $(K_{AF} \cdot J_{F-AF})^{0.5} / M_F$.⁶ The thermally induced reduction of H_E agrees with the aforementioned believed thermally induced reduction of J_{F-AF} . It is likely accompanied by a decrease of K_{AF} in order to counterbalance the measured drop of M_F . The rise of H_C is consistent with reductions of $J_{AF} \cdot M_{AF}$ and K_{AF} , since they both lower AF phases' stability and the more sensitive AF phases consequently become persistently dragged by the F.

Interestingly, the initial positive FC from 750 to 4 K, when all the AF entities are oriented positively, leads to no training (see data point in Fig. 2 for $T_{\text{init}} = 750$ K and $T_a = 4$ K). Conversely, the subsequent negative FC from 750 to 4 K, when all the AF entities are reoriented negatively,

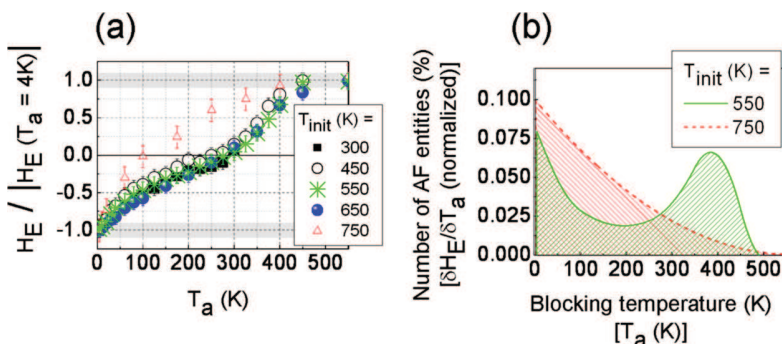


FIG. 4. (a) Comparison of the $H_E/|H_E(T_a = 4 \text{ K})|$ vs T_a variations deduced from Fig. 2. (b) Variations with T_a of the corresponding normalized derivatives $\delta H_E/\delta T_a$ deduced from the full lines in Fig. 2 for $T_{\text{init}} = 550$ and 750 K. $\delta H_E/\delta T_a$ vs T_a represent the blocking temperatures distributions, the integrals of which are set to 100%.

shows training (see data point for $T_a = 750$ K). Although this discrepancy is not fully understood, it can be associated to the use of an *ab initio* positive field which brings about a cause of asymmetry between the above data. It would then point out: (i) that the system tracks memory of the sign of the *ab initio* field; and (ii) that applying a field during deposition can prevent training effects, this latter being in all likelihood sufficient to initially set the AF in a deep enough energy potential well.

To compare the shapes of the H_E vs T_a curves for the various T_{init} , the variations are normalized to their maximum absolute value (for $T_a = 4$ K) and plotted together in Fig. 4(a). Within error bars, the curves overlap for $T_{\text{init}} \leq 650$ K, meaning that the low-T and high-T parts of DT_B related to interfacial spin-glass and grains sizes distributions, respectively, are unchanged, whether the Co/IrMn interface and the grains are as deposited (for $T_{\text{init}} = 300$ K) or annealed. Since DT_B is very sensitive to changes of F and AF properties,⁵⁻¹⁶ one concludes that annealing Co/IrMn bilayers up to slightly below 650 K neither significantly deteriorates the interface by adding more spin-glass phases subsequent to interdiffusions nor the grains by sizes and crystallographic changes. Although the overall shape of the H_E vs T_a curve is not significantly affected, it is noteworthy that the emergence of small training effects for $T_{\text{init}} = 650$ K indicates premises of layers' modifications, which undeniably become manifest for 750 K. Additionally, the discernible slight enhancement of the maximum T_B for $T_{\text{init}} = 650$ K may also well be real. This, as a plausible signature of a grains size increase due to larger T_{init} , cannot be excluded. References 9 and 11 agree that an increase of around 25 K of T_B could result from an increase of around 2 nm of one of the grains' dimensions for typical grain diameters in the range of 5 to 10 nm. Crystallographic changes, for example, leading to strain within grains cannot be discarded either as a possible cause of this potential increase. The derivatives of H_E vs T_a represent the DT_B (Refs. 7 and 9) and are plotted in Fig. 4(b) for $T_{\text{init}} = 550$ and 750 K. The bimodal character of the derivative for $T_{\text{init}} = 550$ K is characteristic of $T_{\text{init}} \leq 650$ K. Interestingly, neglecting training effects by differentiating the H_E vs T_a variations deduced from 1st loops when there is training, e.g., for $T_{\text{init}} = 650$ and 750 K, would lead to an overestimation of the low-T contribution due to spin-glass phases. It is additionally noticeable that the high-T contribution also exists for $T_{\text{init}} = 300$ K, since H_E is due to reach back its maximum of around 800 Oe. However, the maximum pertinent value of T_a is limited by T_{init} , since above T_{init} effects due to DT_B and annealing (when they occur) would mix up, hence making interpretations on DT_B irrelevant. Figure 4(b) shows a clear change from bimodal to unimodal distribution. Only a broad contribution remains at $T_{\text{init}} = 750$ K, which can be ascribed to a shift towards lower T of the high-T contribution. This shift is in concurrence with the aforementioned reductions of AF properties, thus making AF grains sensitive to thermally activated reversal. Such a

shift is possibly driven by a reduction of K_{AF} and also by a decrease of $J_{\text{AF}} \cdot M_{\text{AF}}$ in the core of the grains, but to the extent that Eq. (1) is still fulfilled, since no training was observed for the grains.

To conclude, this study of the influence of annealing on the entire blocking temperature distributions of Co/IrMn bilayers led to different responses, whether grains or spin-glass-like phases were implicated. A better understanding of the respective contributions to EB of grains versus spin-glass was hence provided. Given the diversity of EB stacks and the subsequent large amount of thermally activated layers intermixing, there is a need for systematic comparisons of grains versus spin-glass contributions to EB for many more systems.

This work benefited from useful discussions with B. Dieny, H. Béa, L. Lechevallier, F. Letellier, R. Lardé, and J.-M. Le Breton. B. Dieny is also gratefully acknowledged for the critical reading of the manuscript.

- ¹J. Nogués and I. K. Schuller, *J. Magn. Magn. Mater.* **192**, 203 (1999).
- ²A. E. Berkowitz and K. Takano, *J. Magn. Magn. Mater.* **200**, 552 (1999).
- ³B. Dieny, V. S. Speriosu, S. S. P. Parkin, B. A. Gurney, D. R. Wilhoit, and D. Mauri, *Phys. Rev. B* **43**, 1297 (1991).
- ⁴W. H. Meiklejohn and C. P. Bean, *Phys. Rev.* **102**, 1413 (1956).
- ⁵E. Fulcomer and S. H. Charap, *J. Appl. Phys.* **43**, 4190 (1972).
- ⁶A. P. Malozemoff, *Phys. Rev. B* **35**, 3679 (1987).
- ⁷S. Soeya, T. Imagawa, S. Mitsuoka, and S. Narishige, *J. Appl. Phys.* **76**, 5356 (1994).
- ⁸V. Baltz, J. Sort, B. Rodmacq, B. Dieny, and S. Landis, *Phys. Rev. B* **72**, 104419 (2005).
- ⁹V. Baltz, B. Rodmacq, A. Zarefy, L. Lechevallier, and B. Dieny, *Phys. Rev. B* **81**, 052404 (2010).
- ¹⁰C. K. Safer, M. Chamfrault, J. Allibe, C. Carretero, C. Deranlot, E. Jacquot, J.-F. Jacquot, M. Bibes, A. Barthélémy, B. Dieny, H. Béa, and V. Baltz, *Appl. Phys. Lett.* **100**, 072402 (2012).
- ¹¹K. O'Grady, L. E. Fernandez-Outon, and G. Vallejo-Fernandez, *J. Magn. Magn. Mater.* **322**, 883 (2010).
- ¹²J. Ventura, J. P. Araujo, J. B. Sousa, A. Veloso, and P. P. Freitas, *J. Appl. Phys.* **101**, 113901 (2007).
- ¹³K. Takano, R. H. Kodama, A. E. Berkowitz, W. Cao, and G. Thomas, *Phys. Rev. Lett.* **79**, 1130 (1997).
- ¹⁴M. Ali, P. Adie, C. H. Marrows, D. Greig, B. J. Hickey, and R. L. Stamps, *Nat. Mater.* **6**, 70 (2007).
- ¹⁵F.-T. Yuan, Y. D. Yao, S. F. Lee, and J. H. Hsu, *J. Appl. Phys.* **109**, 07E148 (2011).
- ¹⁶A. G. Biternas, U. Nowak, and R. W. Chantrell, *Phys. Rev. B* **80**, 134419 (2009).
- ¹⁷J. Nogués, J. Sort, V. Langlais, V. Skumryev, S. Surinach, J. S. Munoz, and M. D. Baro, *Phys. Rep.* **422**, 65 (2005).
- ¹⁸M. Gruyters, *Phys. Rev. Lett.* **95**, 077204 (2005).
- ¹⁹F. Letellier, V. Baltz, L. Lechevallier, R. Lardé, J.-F. Jacquot, B. Rodmacq, J.-M. Le Breton, and B. Dieny, *J. Phys. D: Appl. Phys.* **45**, 275001 (2012).
- ²⁰L. Lechevallier, A. Zarefy, F. Letellier, R. Lardé, D. Blavette, J. M. Le Breton, V. Baltz, B. Rodmacq, and B. Dieny, *J. Appl. Phys.* **112**, 043904 (2012).
- ²¹L. Néel, *Ann. Phys. (Paris)* **2**, 61 (1967).
- ²²A. Hoffmann, *Phys. Rev. Lett.* **93**, 097203 (2004).
- ²³C. Binek, *Phys. Rev. B* **70**, 014421 (2004).
- ²⁴B. Beschoten, J. Keller, A. Tillmanns, and G. Güntherodt, *IEEE Trans. Magn.* **38**, 2744 (2002).